# Path Planning Based on Dimension Reduction and Region Clipping for Aircraft Fuel Tank Inspection Robot

Qingji Gao
Robotics Institute/Civil Aviation University of China, Tianjin, China
Email: qjgao@cauc.edu.cn

Zunchao Zheng and Guochen Niu
Robotics Institute/Civil Aviation University of China, Tianjin, China
Email: zc.zheng.leon@gmail.com, niu_guochen@139.com

***Abstract*—A continuum robot for inspecting aircraft fuel tank is designed to improve the performance of manual maintenance. Path planning for this kind of robot is challenging due to their complex kinematics models. In an environment without obstacles, a strategy of path planning is proposed in this paper. Dimension reduction method is presented and an imaginary straight line between the starting point and the target is made up as a reference line to simplify the problem. A novel search method based on region clipping deduced from continuity analysis of position function is proposed to decrease computing time complexity. Minimum distance summation (MDS) is calculated to decide the optimal path relatively. Simulation results and analysis demonstrate excellent performance of region clipping search method and feasibility of path planning.**

***Index Terms*—continuum robot, path planning, region clipping, dimension reduction, aircraft fuel tank inspection**

## I. Introduction

Aircraft fuel tank is such an environment that is complicated and narrow enough to be inspected uncomfortably for aircrews, since it distributes uniform stringers, fuel pipes and related facilities in disorder and is full of kinds of toxic gases. The crews must follow the intricate AMM (Aircraft Maintenance Manual) strictly in order to increase personnel security, so a semi-automatic device is in urgent need to improve maintenance efficiency and reduce labor intensity. As shown in Fig. 1, an aircraft fuel tank inspection robot (AFTIR) with continuous structure to assist the crews in carrying out inspection operations is designed in this paper.

Qingji Gao, Robotics Institute, Civil Aviation University of China, Tianjin 300300 China, email: qjgao@cauc.edu.cn.
Zunchao Zheng, Robotics Institute, Civil Aviation University of China, Tianjin 300300 China, email: zc.zheng.leon@gmail.com.
Guochen Niu, Robotics Institute, Civil Aviation University of China, Tianjin 300300 China, email: niu_guochen@139.com.

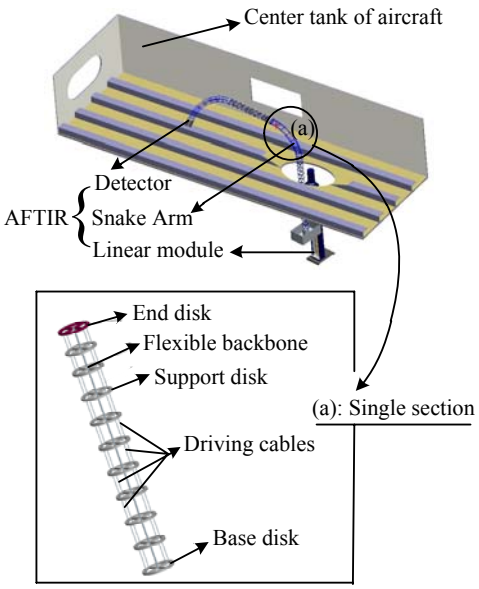


Figure 1. Pro-E simulation of aircraft fuel tank inspection robot (AFTIR) entering aircraft center tank for inspecting and (a) is the partial diagram of single section of Snake Arm.

Continuum robot, which has such biological features as snakes, elephant trunks and octopus arms, can vary in shape and size to adapt to the environment with strong space constraints like aircraft fuel tank. Some types of continuum robots have been designed, such as OCRobotics [1], DDU [2], Air-Octor [3], OctArm [4], Active Cannulas [5], Colobot [6], BHA [7], etc. In order to achieve the target in a cluttered space, path planning needs to be studied. Work has been done for continuum robots moving from the starting point to the target zone. G. S. Chirikjian *et al.* model hyper-redundant rigid link robots using parametric curves approximated by mode shape function (MSF) which is modified to apply to continuum robot [8]. I. S. Godage *et al*. present a MSFs-based kinematic model, avoiding the complex derivations and singularities [9-11]. Simulations of forward


doi:10.4304/jsw.9.6.1626-1633

kinematics, position inverse kinematics with and without orientation, object inspection and handling, motions in static and dynamic environments demonstrate spatial bending, pure elongation/contraction and ability of avoiding obstacle. W. Park *et al*. formulate the steering problem for a flexible needle as a nonholonomic kinematics problem [12]. V. Duindam *et al.* propose a 3D motion planning method for a bevel-tip flexible needle in an environment with obstacles [13]. The planning problem is expressed as an optimization problem by discretizing control space and the discretization includes a stop-and-turn strategy and a helical strategy. But there may be no solutions for different initial estimates. The needle-tip pose probabilities generated as a diffusion process on the Euclidean group are studied. Based on Rapidly-Exploring Random Trees (RRTs) method, J. J. Xu *et al*. develop a motion planner for steerable needles in 3D environment with obstacles [14]. They also propose a method using RRTs with backchaining to solve the possible problem of no solutions for all given initial configurations. L. A. Lyons *et al.* present a motion planning algorithm based on optimization for an active cannula reaching the target while avoiding obstacles [15]. Penalty methods are used to solve the constrained nonlinear optimization problem by converting it into a sequence of unconstrained optimization problems. J. Xiao *et al.* design a real-time adaptive motion planner (RAMP) for a multisection trunk/tentacle robot to grasp an object under uncertain conditions [16]. It uses a planar curve parametric kinematic model to the extended RAMP paradigm.

Researches aforementioned provide path planning methods for a variety of continuum robots, but they cannot be applied directly to AFTIR due to primary differences in physical mechanisms and relative kinematics models. This paper aims to plan a feasible path for AFTIR by searching solutions of fundamental kinematics using a novel method of region clipping. We emphasize the improvement of search process since the original blind search method is time-consuming numerously. In addition, the planning problem is also simplified by introducing dimension reduction and reference straight line.

The structure of this paper is as follows. Section II presents the related fundamental work including mechanical structure and kinematics model we have studied on the AFTIR [17]. Section III defines the problem of path planning and section IV details the main idea of dimension reduction strategy, region clipping search method and planning strategy. And analysis of simulation results follows in section V.

## II. PRELIMINARIES

### A. Overviews of Mechanical Structure

As shown in Fig.1, the structure of AFTIR mainly consists of three parts: the detector, Snake Arm and linear module. The detector percepts the environment using CCD camera, the flexible Snake Arm enters the interior of the fuel tank for inspection, and rigid linear module, the external part of fuel tank supports and provides rising and falling movements of Snake Arm. The arm consists of several continuous sections. The structure of single section is shown as in the part (a) of Fig. 1. Each section consists of some support disks, driving cables and one flexible backbone, and it can bend and rotate through changing lengths of four driving cables which are uniformly distributed around backbone at intervals of 90°.

### B. Overviews of Kinematics Model

Through the analysis of kinematics of single section and multi-sections [17], a mapping relationship between the joint variables and tip position vector of N sections is established. The homogeneous transformation matrix (HTM) of tip frame {N} relative to system frame {0} can be expressed by (1).

$$ {}^{0}_{N}\boldsymbol{T} = {}^{0}_{1}\boldsymbol{T} \cdots {}^{i-1}_{i}\boldsymbol{T} \cdots {}^{N-1}_{N}\boldsymbol{T} \tag{1} $$

Where, ${}^{i-1}_{i}\boldsymbol{T}$ is the section frame {i} relatives to that of {i-1}, it is a 4×4 matrix and given by (2).

$$ {}^{i-1}_{i}\boldsymbol{T}_{4\times4} = \begin{bmatrix} {}^{i-1}_{i}\boldsymbol{R}_{3\times3} & {}^{i-1}_{i}\boldsymbol{p}_{1\times3}{}^{T} \\ 0 & 1 \end{bmatrix} \tag{2} $$

Where, ${}^{i-1}_{i}\boldsymbol{R}$ is the rotation matrix, it is a 3×3 matrix. ${}^{i-1}_{i}\boldsymbol{p}^{T}$ is the position of the origin in frame {i} relative to that in frame {i-1}, it is a 1×3 vector. The elements of ${}^{i-1}_{i}\boldsymbol{T}$ are functions of bending angle $\theta_i$ and rotation angle $\square_i$ of i# section.

## III. PROBLEM STATEMENT

Continuum robot is a kind of robot that differs from car-like robots which can be taken as particles when planning a path from the starting point to the target, flexibility of single section and correlation between sections result in that the path planning is not as easy as that for a particle. For this reason, we define path planning for continuum robot as follows.

***Definition:*** Plan a feasible path from a starting point to the target zone and make the final pose of continuum robot as the planned path of continuum robot.

With the above definition, the path planning for AFTIR can be stated as follows.

***Problem:*** Given a target point, the starting position and orientation, determine a feasible strategy that makes AFTIR reach the target zone, make sure that positions of endpoints and tip point of the body are known (the tip point is the final endpoint of the end section of Snake Arm), and promise that the body of Snake Arm does not collide with boundaries of fuel tank.

***Input:*** Workspace simulating the structure of aircraft fuel tank, entry configuration of continuum robot, the target point $P_{target}$ which the robot required to reach.

***Output:*** Joint variables including the bending and rotation angles of all sections and the rising distance, or

'Cannot reach the target' is reported.

## IV. METHODOLOGY

### A. Dimension Reduction

Fuel tank is a 3D environment, and for a target in space, there are more than one feasible solutions with the forward kinematics model, that is, there are multi-paths from the starting point to a target as shown in Fig. 2(a) in which there are *path1* of five sections and *path2* of four sections in space for the same target, and their projections in plane *XOY* are different curves. Multi-solutions bring about high computing time complexity and difficulty of choosing the optimal path, especially when we have to make the searching step smaller to obtain more accurate solutions. To solve the above problems, a method based on dimension reduction is proposed through transforming path planning in 3D space to that in 2D plane. As shown in Fig. 2(b), in the plane γ, we get a path whose projection is a planar straight line from original point to the projective point of target in plane *XOY*. From the kinematics model of multi-sections, we know that rotation angles of all the sections of Snake Arm are the same □, which can be calculated by (3), if the position coordinates of target is $\boldsymbol{p}=[x_t,y_t,z_t]$. In this way, solutions calculated in 3D space are transferred to that in 2D plane.

$$\phi = \arctan\left(\frac{y_t}{x_t}\right), x_t \neq 0 \tag{3}$$

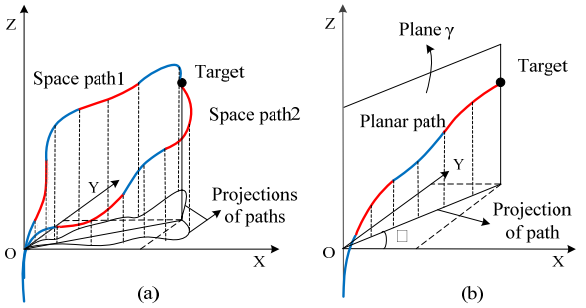


Figure 2. Diagram of paths in 3D space (a) and 2D plane (b)

The rising distance will be calculated by dimension reduction method. Firstly, the initial configuration is a status that the base of Snake Arm is on the original point in frame and perpendicular to plane *XOY*. Then the arm bends until the tip point $P_{tip}$ moves into the target zone, a target zone is determined by projection distance from $p_{tip}$ to $p_{target}$ ($p_{tip}$ and $p_{target}$ are respectively the projections of $P_{tip}$ and $P_{target}$ on plane *XOY*) given by (4). Finally, the arm poses satisfying conditions of reaching target zone moves a rising distance upward or downward until the tip point goes into the horizontal plane in which the target point locates, in this way, the final pose is the desired path and the rising distance is obtained at the same time.

$$|\Delta p| = |p_{tip} - p_{target}| \tag{4}$$

### B. Region Clipping

The main idea comes from the analysis of continuity of functions based on forward kinematics, and dimension reduction strategy mentioned above is the precondition of the analysis of the method.

For a single section in path planning with dimension reduction, the known rotation angle of a single section in path planning with dimension reduction is defined as $\phi_0$ which is constant. And for an arbitrary unknown variable of bending angle $\theta$, define $\boldsymbol{p}_{Nr}$ ($N$ is the number of sections, $N$=1 here means the arm is a single section, $r$ represents a distance from a point on the section to the base of the section, $r \geq 0$ and $r \leq l$) as an arbitrary point on the body and the corresponding bending angle is $\alpha$. So, the position vector of $\boldsymbol{p}_{1r}=[x_{1r},y_{1r},z_{1r}]$ is given by $\boldsymbol{p}_{Nr}=[x_{Nr},y_{Nr},z_{Nr}]$ ($N$=1) and where

$$\begin{cases} x_{1r} = \dfrac{l}{\theta}\cos(\phi_0)(1-\cos(\alpha)) \\ y_{1r} = \dfrac{l}{\theta}\sin(\phi_0)(1-\cos(\alpha)) \\ z_{1r} = \dfrac{l}{\theta}\sin(\alpha) \\ \alpha = \dfrac{r}{l}\bullet\theta \\ \theta \neq 0 \end{cases} \tag{5}$$

It indicates in (5) that, $\phi_0$ is known as constant, so $x_{1r}$, $y_{1r}$, $z_{1r}$ are taken as unary functions of $\theta$, moreover, they are also complex functions of multiple elementary functions. If $\theta$ tends to zero, that is, $\alpha$ tends to zero, we have (6).

$$\begin{cases} \lim\limits_{\theta\to 0} x_{1r} = 0 = x_{1r}(\theta)|_{\theta=0} \\ \lim\limits_{\theta\to 0} y_{1r} = 0 = y_{1r}(\theta)|_{\theta=0} \\ \lim\limits_{\theta\to 0} z_{1r} = l = z_{1r}(\theta)|_{\theta=0} \end{cases} \tag{6}$$

The definition of continuity of unary function indicates that elementary functions $x_{1r}$, $y_{1r}$, $z_{1r}$ are continuous functions [18], that is, position function of single section is continuous for $\theta$ in interval of $[-\pi,\pi]$.

For multi-sections, rotation angle $\phi_i$ ($i$=1,2,…,$N$) can be treated as constant when employing dimension reduction strategy, and they are equivalent to each other, $\phi_i=\phi_0$, where $\phi_0$ is calculated by (3). Then we can take each element of ${}^{i-1}_{i}\boldsymbol{T}$ as a unary function of $\theta$ given by (7), where $c$ and $s$ are respectively short for trigonometric functions of *cos* and *sin*. The conclusions above-mentioned imply that each of the sixteen functions ${}^{i-1}_{i}f_{mn}(\theta_i)$ ($m$=1,2,3,4 and $n$=1,2,3,4) is continuous for $\theta_i$ in interval of $[-\pi,\pi]$.

As ${}^{0}_{N}\boldsymbol{T}$ in (2) is got by a product of $N$ matrices, $\boldsymbol{p}_{Nl}$ is formulated through the multiplications and additions of elements of $N$ matrices. For a combination $\{\theta_1,\ldots,\theta_N\}$, we choose $\theta_i$ arbitrarily as an independent variable $\theta$ and then the others in $\{\theta_1,\ldots,\theta_{i-1},\theta_{i+1},\ldots,\theta_N\}$ are constants. In this way, (2) can be given by (8).

$$ {}^{i-1}_{i}\boldsymbol{T}=\begin{bmatrix} c^2\phi_0 c\theta_i+s^2\phi_0 & c\phi_0 s\phi_0 c\theta_i-c\phi_0 s\phi_0 & c\phi_0 s\theta_i & \frac{l}{\theta_i}\mathrm{c}\,\phi_0(1-c\theta_i) \\ c\phi_0 s\phi_0 c\theta_i-c\phi_0 s\phi_0 & s^2\phi_0 c\theta_i+c^2\phi_0 & s\phi_0 s\theta_i & \frac{l}{\theta_i}s\phi_0(1-c\theta_i) \\ -c\phi_0 s\theta_i & -s\phi_0 s\theta_i & c\theta_i & \frac{l}{\theta_i}s\theta_i \\ 0 & 0 & 0 & 1 \end{bmatrix}=\begin{bmatrix} {}^{i-1}_{i}f_{11}(\theta_i) & {}^{i-1}_{i}f_{12}(\theta_i) & {}^{i-1}_{i}f_{13}(\theta_i) & {}^{i-1}_{i}f_{14}(\theta_i) \\ {}^{i-1}_{i}f_{21}(\theta_i) & {}^{i-1}_{i}f_{22}(\theta_i) & {}^{i-1}_{i}f_{23}(\theta_i) & {}^{i-1}_{i}f_{24}(\theta_i) \\ {}^{i-1}_{i}f_{31}(\theta_i) & {}^{i-1}_{i}f_{32}(\theta_i) & {}^{i-1}_{i}f_{33}(\theta_i) & {}^{i-1}_{i}f_{34}(\theta_i) \\ {}^{i-1}_{i}f_{41}(\theta_i) & {}^{i-1}_{i}f_{42}(\theta_i) & {}^{i-1}_{i}f_{43}(\theta_i) & {}^{i-1}_{i}f_{44}(\theta_i) \end{bmatrix} \tag{7} $$

$$ {}^{0}_{N}\boldsymbol{T}(\theta)={}^{0}_{1}\boldsymbol{T}(\theta_1)\cdots{}^{i-2}_{i-1}\boldsymbol{T}(\theta_{i-1})\bullet{}^{i-1}_{i}\boldsymbol{T}(\theta)\bullet{}^{i}_{i+1}\boldsymbol{T}(\theta_{i+1})\cdots{}^{N-1}_{N}\boldsymbol{T}(\theta_N) \tag{8} $$

We take elements of ${}^{0}_{N}\boldsymbol{T}$ as functions ${}^{0}_{N}f_{mn}(\theta)$ ($m$=1,2,3,4; $n$=1,2,3,4), the subscript $mn$ represents its position of the matrix ${}^{0}_{N}\boldsymbol{T}$, the $m$-th row and $n$-th column. From (2), $\boldsymbol{p}_{Nl}$ can be given by (9).

$$ \begin{aligned} \boldsymbol{p}_{Nl}&=[x_{Nl},y_{Nl},z_{Nl}] \\ &=\left[{}^{0}_{N}f_{14}(\theta),\ {}^{0}_{N}f_{24}(\theta),\ {}^{0}_{N}f_{34}(\theta)\right] \end{aligned} \tag{9} $$

Where ${}^{0}_{N}f(\theta)$ can be regarded as unary function of $\theta$ through operation combinations of elements of ${}^{j-1}_{j}\boldsymbol{T}$ ($j$=1,2,…,$N$), as given by (10). Obviously, $\theta$ is continuous in [-π,π].

$$ \begin{aligned} &{}^{0}_{N}f_{kj}(\theta)= \\ &g\left[{}^{0}_{1}f_{mn}(\theta_1),\cdots,{}^{i-2}_{i-1}f_{mn}(\theta_{i-1}),{}^{i-1}_{i}f_{mn}(\theta),{}^{i}_{i+1}f_{mn}(\theta_{i+1}),\cdots,{}^{N-1}_{N}f_{mn}(\theta_N)\right] \\ &k=1,2,3;\quad j=4;\quad m=1,2,3,4;\quad n=1,2,3,4 \end{aligned} \tag{10} $$

Where $g(\bullet)$ is a function of $\theta$ with an operation combination of elements of ${}^{j-1}_{j}\boldsymbol{T}$ ($j$=1,2,…,$N$), this kind of combination is an elementary operation of multiplications and additions of ${}^{i-1}_{i}f_{mn}(\bullet)$ ($i$=1,2,…,$N$) which represents any element of ${}^{i-1}_{i}\boldsymbol{T}$.

By the definition of continuous unary function in [18], we could imply from (10) as follows.

$\forall\varepsilon>0$, $\exists\Delta\theta>0$, s.t $\left|{}^{0}_{N}f_{kj}(\theta)-{}^{0}_{N}f_{kj}(\theta_0)\right|<\varepsilon$, for $\forall\theta\in O(\theta_0,\Delta\theta)$.

In another way, for $\theta_0$ ($\theta_0$ is the value of bending angle of $i$# section, with a known combination { $\theta_1$, …,$\theta_{i-1}$, $\theta_{i+1}$,…,$\theta_N$ } and $\theta_0$) corresponds a target point $[x_{Nl}(\theta_0),y_{Nl}(\theta_0),z_{Nl}(\theta_0)]$ which is in target zone, when the variable $\theta$ changes by $\Delta\theta$ and $\Delta\theta$ tends to zero, we obtain conclusions as (11).

$$ \begin{cases} \lim\limits_{\Delta\theta\to0}\Delta x_{Nl}=0 \\ \lim\limits_{\Delta\theta\to0}\Delta y_{Nl}=0 \\ \lim\limits_{\Delta\theta\to0}\Delta z_{Nl}=0 \end{cases} \tag{11} $$

So the position change $\Delta d$ on the direction of vector $[\Delta x_{Nl},\Delta y_{Nl},\Delta z_{Nl}]$ is calculated by (12).

$$ \begin{aligned} \lim_{\Delta\theta\to0}|\Delta d|&=\left|\sqrt{\Delta x_{Nl}{}^2+\Delta y_{Nl}{}^2+\Delta z_{Nl}{}^2}\right| \\ &=\sqrt{\lim_{\Delta\theta\to0}\Delta x_{Nl}{}^2+\lim_{\Delta\theta\to0}\Delta y_{Nl}{}^2+\lim_{\Delta\theta\to0}\Delta z_{Nl}{}^2} \\ &=0 \end{aligned} \tag{12} $$

Combining (11) and (12), we learn that when $\theta$ changes nearby $\theta_0$, the tip point moves nearby point $[x_{Nl}(\theta_0),y_{Nl}(\theta_0),z_{Nl}(\theta_0)]$, that is, the tip point changes near the target zone in a direction from [0,0,0] to $[\Delta x_{Nl},\Delta y_{Nl},\Delta z_{Nl}]$.

In conclusion, continuity means the position coordinates of $\boldsymbol{p}_{Nl}$ are distributed continuously in each coordinate axis orientation, or, continuity analysis of unary functions presents relations between changes of bending angles and movements of tip point, that is, the position of tip point changes gradually, other than mutationally. In another way, if a solution is gained, in which the tip point occurs in the target zone, through changing angles a more suitable solution near the above known angles can be achieved until the optimal one is found and tip point is not out of target zone.

When the blind search is applied, it searches many useless angles, which leads to large computing time. To reduce computing time, considering the distribution of useful values, a search method of region clipping is presented. The main idea comes from the analysis of continuity of HTM, and it aims to reserve useful region and remove the useless regions through searching less values continually. As shown in Fig. 3, firstly we divided the interval of $\theta$ into NUM parts averagely and get (NUM+1) values in the searching region (NUM is usually a small integer, in Fig. 3, NUM=6), and we get a series of combinations $\{\theta_i(1),\ldots,\theta_i(7)\}$ for i# section. Through calculating the tip coordinates is calculated, if the condition of reaching the target zone is satisfied, keep the values. Secondly, we choose an optimal value $\{\theta_1(5),\ldots,\theta_N(3)\}$ which is calculated from minimum distance summation (MDS) which is the summation of distances from all points of Snake Arm to a reference straight line, and make its prior value $\{\theta_1(4),\ldots,\theta_N(2)\}$ and its later one $\{\theta_1(6),\ldots,\theta_N(4)\}$ as left and right endpoints of the next searching regions. Finally, the loop stops when the computed MDS remains unchanged. In this way, 6 of 7 values will be abandoned in the next loop. Just like a tailor, most of searching regions are clipped in each loop until the optimal value obtained so that a large amount of unnecessary values will not be calculated and a low

computing time complexity will be got.

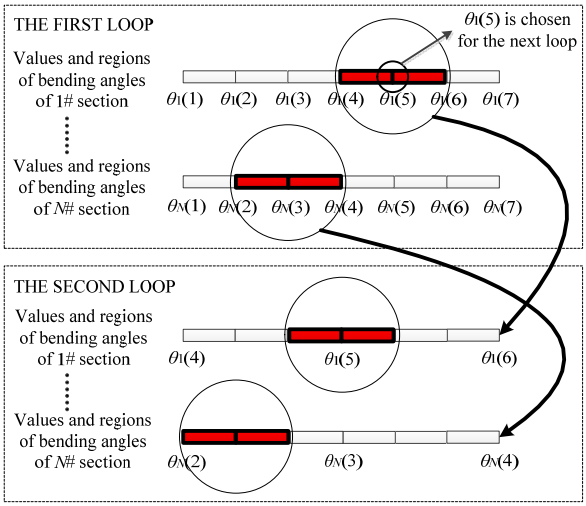


Figure 3. Principle of region clipping search method and the red regions are reserved in each loop.

### C. Planning Algorithm

Imagining there is a straight line between original point and target point, clearly, in a 3D space without obstacles, the optimal path from the starting point to the target point is the straight line. But in consideration of characteristics of continuum robot, we use the fictitious line as reference and adopt a planning method based on dimension reduction and region clipping, and obtain the optimal result through calculating MDS. The main algorithm details as follows.

Initialize the configurations, as shown in TABLE I.

TABLE I.

PROGRAMING DESIGN OF PATH PLANNING

| PLANNING_PROCEDURE(Pinit,Ptarget) |
|---|
| 1. DEFINE $O_{target}$ as a target zone |
| 2. DRAW_REFERENCE_LINE($P_{init}$,$P_{target}$) |
| 3. CALCULATE number of sections N |
| 4. DIVIDE regions of $\theta_1,\ldots, \theta_N$ |
| 5. OBTAIN Θ combined of $\{ \theta_1,\ldots, \theta_N \}$ |
| 6. while MDSs in adjacent loop are not equal |
| 7. for all $\{ \theta_1,\ldots, \theta_N \}$ □Θ |
| 8. CALCULATE the tip point $S_{target}$ |
| 9. while $S_{target} \cap O_{target} \neq \varnothing$ |
| 10. CALCULATE the MDSs |
| 11. GENERATE set of Θ |
| 12. END |
| 13. RETURN optimal $\{ \theta_1,\ldots, \theta_N \}$ and rising distance |

Input the starting point $P_{init}$ and the target point $P_{target}$. Draw the reference straight line from $P_{init}$ to $P_{target}$. For $P_{init}$, we calculate the number of sections $N$. For $\theta_i$ corresponding the i# section, we divide its domain into NUM parts, then a set of Θ composed of all combinations of $\{\theta_1,\ldots,\theta_N\}$ is formed. For each element of Θ, a set of tip points which satisfy the condition of reaching target zone are calculated. There is a corresponding summation of distances from discrete points along the section to the reference straight line for every combination $\{\theta_1,\ldots, \theta_N\}$ of tip points, and the minimum one of the group of summations is calculated, that is MDS. When the MDS is approximate to the MDS got from former loop, the loop stops and corresponding joint variables and rising distance are returned.

## V. Simulation Results and Analysis

### A. Performance of Region Clipping

A series of simulations are carried out in order to validate performance in reducing computing time complexity and feasibility of region clipping search method. As shown in TABLE II, we list three groups of comparison experiments between blind search method and proposed search method, where T represents the type of method (A and B represent blind search and the region clipping based method respectively), $N$ is the number of active sections, $\theta_i$ ($i$=1,…,4) is bending angle, $d$ is the rising distance of linear module, *loops* is the number of loops, *time* means the running time. For experiments of blind search, we set the length of single section $l$=25cm, the searching step of bending angle $\Delta\theta$=1°, the planner distance of determining limits of reaching the target $|\Delta p|<$ 0.5cm. In simulations of novel search method, we divide the searching region of each section into 9 subintervals equally, and 10 values of each section partake the searching, so that we get the best one to make up a new searching region with its former and later values and the others will not be calculated in the next loop. Fig. 4 shows the intervals contraction process of two sections in each loop of region clipping search method, intervals of $\theta_1$ and $\theta_2$ form a square search region in first loop, and the region become $(7/9)^2$ smaller than that in the next loop until the final solution is obtained, and the final solution is the optimal $\theta_1$ and $\theta_2$ we desire. Similarly, the process of three sections is shown in Fig. 5. The poses of three solutions by blind search in TABLE II are shown in Fig.6 (a1), (a2) and (a3) successively and the corresponding ones by region clipping are shown in in Fig.7 (b1), (b2) and (b3) successively, where the pink line represents the reference straight line, the blue one is the pose of arms whose tip reaching the target, and the red point on the blue curve is the endpoint of each section.

The computing complexity of blind search is $O(N^K)$ (K is the number of search steps and determined by the length of search step), and that of region clipping is $O((NUM+1)^N)$ (NUM=9). For blind search, the shorter the length of step, the better the solution is, so K is usually a big number. By analysis of the comparisons in TABLE II, we conclude that there is a large improvement in performance of time consuming with presented search method. It is important especially for yielding the solutions of multiple sections as formula of multi-section

model is more complex. From Fig. 6 and Fig. 7, we know the optimal solutions under the conditions of reaching the target zone and obtaining the MDSs are similar between two search methods, that is, the values got from region clipping search method are reasonable.

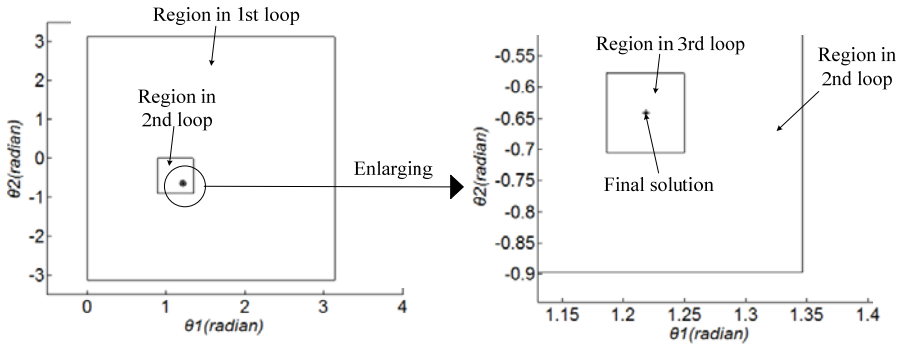


Figure 4. Searching regions changes in three loops using region clipping method until the optimal solution of two sections is obtained, there are three loops in all, searching region keeps reducing, every reduction are $(7/9)^2$ of the former region.

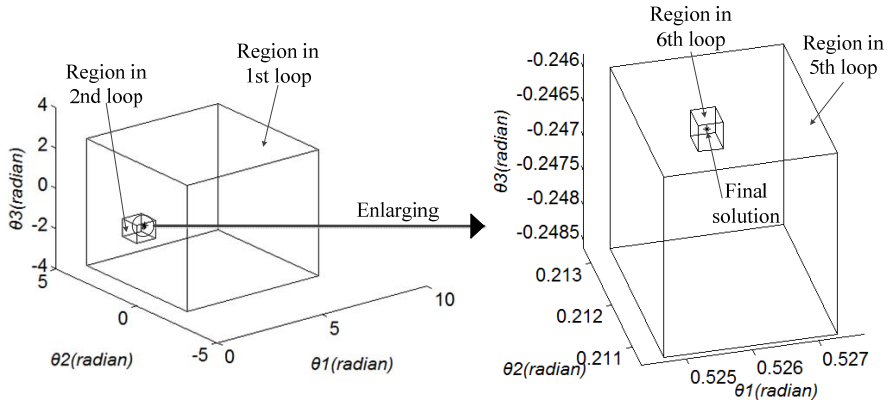


Figure 5. Searching regions changes of six loops using region clipping method until the optimal solution of three sections is obtained, there are six loops in all, searching region keeps reducing, every reduction are $(7/9)^3$ of the former region, the middle process is ignored in the figure.

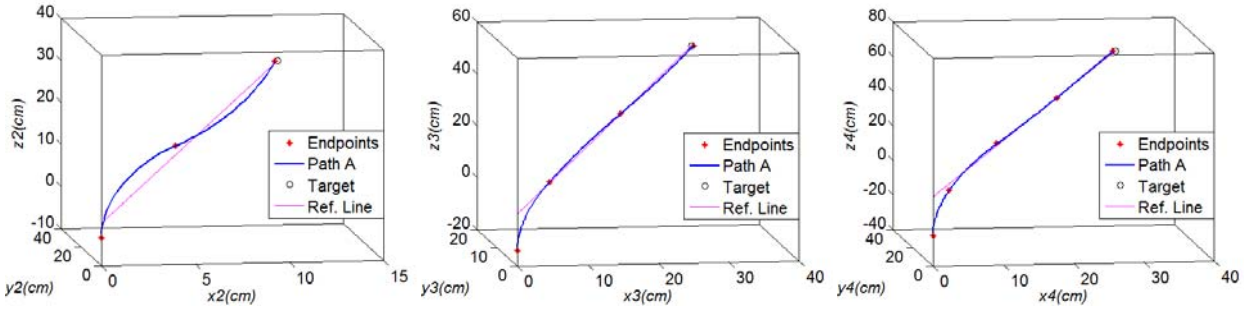


Figure 6. Using blind search method, we obtain solutions of two, three and four sections, as shown respectively in figure (a1), (a2) and (a3).

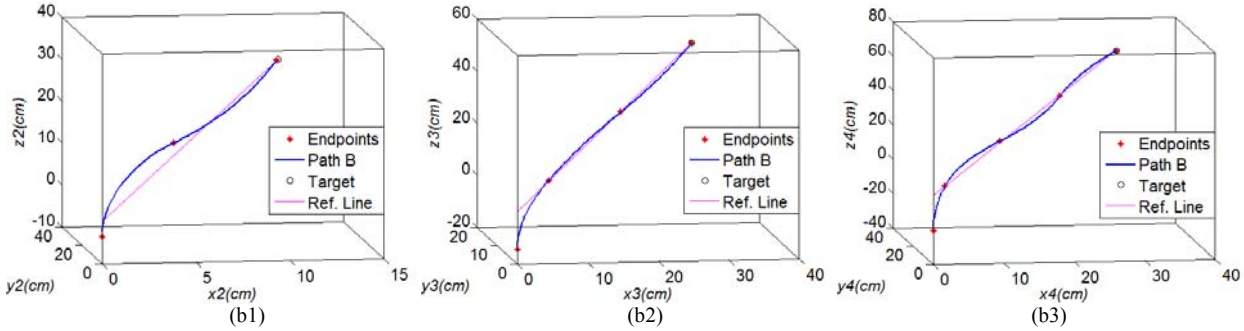


Figure 7. Using region clipping search method, we obtain solutions of two sections (b1), three sections (b2) and four sections (b3), they correspond respectively to (a1), (a2) and (a3) in Figure.6.

TABLE II.

SOLUTIONS OF 2-4 SECTIONS WITH DIFFERENT SEARCH METHODS

| | T | *N* | Target [x,y,z](cm) | $\{\theta_1,\ldots,\theta_N\}$ (radian) | *d*(cm) | *loops* | *time* |
|---|---|---|---|---|---|---|---|
| 1 | A | 2 | [11,31,31] | {1.27, -0.82} | -3.51 | $8.8\times10^3$ | 0.58s |
| 2 | B | | | {1.22, -0.64} | -3.58 | $3.0\times10^2$ | 0.09s |
| 3 | A | 3 | [30,19,50] | {0.53, 0.17, -0.12} | -14.18 | $3.3\times10^5$ | 26.62s |
| 4 | B | | | {0.53, 0.21, -0.25} | -14.39 | $6.0\times10^3$ | 0.96s |
| 5 | A | 4 | [30,29,67] | {0.24, 0.54, -0.42, 0.40} | -20.91 | $1.7\times10^7$ | 31 min |
| 6 | B | | | {0.21, 0.66, -0.55, 0.46} | -20.61 | $4.0\times10^4$ | 6.88s |

### *B. Improvement of Region Clipping*

Region clipping requires ignoring many searching regions, but the optimal solution depending on MDS may be skipped over in one loop, and the solution solved by next loops will be larger than the optimal one. We can optimize the problem by changing the number of subintervals NUM and the boundaries of searching regions. As shown in Fig. 8, there are two paths of five sections for a target [40,59,77], the final MDS of Path One is 76.80cm, and that of Path Two is 65.27cm, clearly it is smaller than the former one. Or we can conclude that the final path can be optimized by the change of parameters related to searching region.

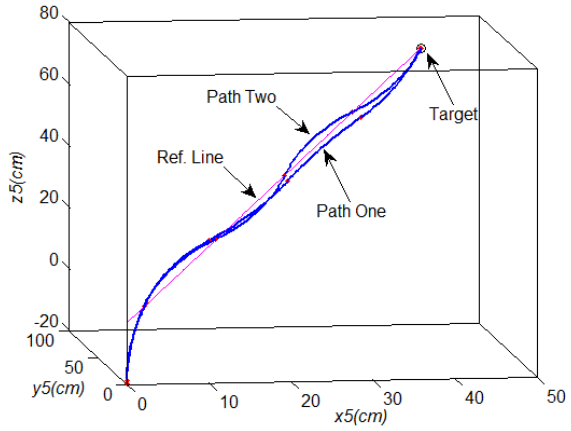


Figure 8. Different solutions of five sections to find the optimal path through changing parameters.

### *C. Application in Fuel Tank*

In order to apply this path planning algorithm to the fuel tank, the center tank of aircraft sized by Boeing 737 is also simulated. Eight special positions are chosen, and if we can reach these vertexes which represent utmost distances in eight quadrants, we can achieve any target in the tank. And the coordinates of eight targets in TABLE III correspond that in Fig. 9 which shows the positions and relative solutions we get finally. The simulations demonstrate the feasibility of applications in the aircraft fuel tank using the proposed path planning algorithm.

TABLE III.

EIGHT POSITIONS OF THE TANK USED FOR THE SIMULATION IN FIGURE 9.

| No. | Position coordinates(cm) |
|---|---|
| 1# | [-43.5, -60.2, 0] |
| 2# | [-43.5, -60.2, 97] |
| 3# | [42.5, -60.2, 0] |
| 4# | [42.5, -60.2, 97] |
| 5# | [-43.5, 301.6992, 0] |
| 6# | [-43.5, 301.6992, 97] |
| 7# | [42.5, 301.6992, 0] |
| 8# | [42.5, 301.6992, 97] |

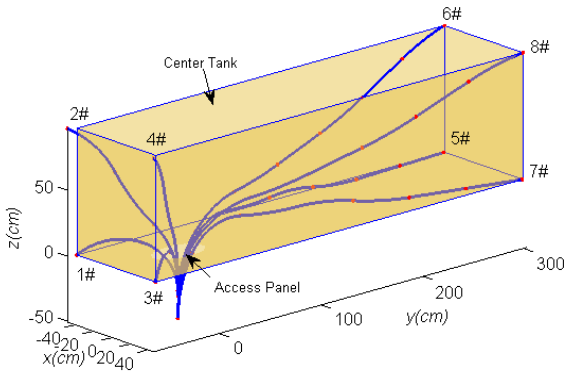


Figure 9. Simulations of paths for eight targets of the center tank, the eight blue lines are the planned paths, the red points are endpoints of sections and the length of single section is 50cm here.

## VI. CONCLUSIONS AND FUTURE WORK

The purpose of this paper is to plan a feasible path as quickly as possible for AFTIR in an environment without obstacles. Before the work, path planning of continuum robot is defined. An improvement on search method is made, and the method based on region clipping which is deduced from the analysis of continuity of unary position functions is presented to reduce computing time complexity. Simulation results display the prominent performance of the novel method. When it comes to path planning strategy, we make a fictitious line as an reference object between the original point and the target point. To reduce the complexity of solving multi-solutions, dimension reduction strategy is proposed through simplifying the 3D problem to a 2D planning. Under the conditions of reaching the target zone, the results are optimized by calculating MDS. Simulations of region clipping and path planning algorithm are carried out to demonstrate excellent performance of the novel search method and feasibility of path planning strategy.

In future work, we plan to emphasize the work on two

aspects. On one hand, we will try to apply the region clipping search method to the obstacle avoidance path planning in a cluttered space. On the other hand, practical experiments of prototype to test and verify the algorithms will be taken into account.

## ACKNOWLEDGMENT

This work was supported by Robotics Institute of Civil Aviation University of China.

## REFERENCES

[1] R. Buckingham, "Snake arm robots," *Industrial Robot: An International Journal*, vol. 29, no.3, pp. 242-245, 2002.
[2] N. Simaan, "Snake-like units using flexible backbones and actuation redundancy for enhanced miniaturization," in *Proc. IEEE Int. Conf. on Robotics and Automation*, Barcelona, 2005, pp. 3012-3017.
[3] W. McMahan, B. A. Jones, and I. D. Walker, "Design and implementation of a multi-section continuum robot: Air-Octor," in *Pro. IEEE/RSJ Int. Conf. on Intelligent Robots and Systems*, Edmonton, 2005, pp. 3345-3352.
[4] W. McMahan, B. A. Jones, V. Chitrakaran, M. Csencsits, M. Grissom, M. Pritts, C. D. Rahn, and I. D. Walker, "Field trials and testing of the OctArm continuum manipulator," in *Proc. IEEE Int. Conf. on Robotics and Automation*, Orlando, 2006, pp. 2336-2341.
[5] R. J. Webster III, A. M. Okamura, and N. J. Cowan, "Toward active cannulas: miniature snake-like surgical robots," in *Proc. IEEE/RSJ Int. Conf. on Intelligent Robots and Systems*, Beijing, 2006, pp. 2857-2863.
[6] G. Chen, M. T. Pham, and T. Redarce, "Development and kinematic analysis of a silicone-rubber bending tip for colonoscopy," in *Proc. IEEE/RSJ Int. Conf. on Intelligent Robots and Systems*, Beijing, 2006, pp. 168-173.
[7] M. Rolf and J. J. Steil, "Constant curvature continuum kinematics as fast approximate model for the bionic handling assistant," in *2012 IEEE/RSJ Int. Conf. on Intelligent Robots and Systems*, pp. 3440-3446.
[8] G. S. Chirikjian and J. W. Burdick, "An obstacle avoidance algorithm for hyper-redundant manipulators," in *1990 IEEE Int. Conf. on Robotics and Automation*, pp. 625–631 vol.1.
[9] I. S. Godage, D. T. Branson, E. Guglielmino, G. A. Medrano-Cerda, and D. G. Caldwell, "Shape function-based kinematics and dynamics for variable length continuum robotic arms," in *2011 IEEE Int. Conf. on Robotics and Automation*, pp. 452–457.
[10] I. S. Godage, E. Guglielmino, D. T. Branson, G. A. Medrano-Cerda, and D. G. Caldwell, "Novel modal approach for kinematics of multisection continuum arms," in *2011 IEEE/RSJ Int. Conf. on Intelligent Robots and Systems*, pp. 1093–1098.
[11] I. S. Godage, D. T. Branson, E. Guglielmino, and D. G. Caldwell, "Path planning for multisection continuum arms," in *Proc. IEEE Int. Conf. on Mechatronics and Automation*, Chengdu, 2012, pp. 1208-1213.
[12] W. Park, J. S. Kim, Y. Zhou, N. J. Cowan, A. M. Okamura, and G. S. Chirikjian, "Diffusion-based motion planning for a nonholonomic flexible needle model," in *Proc. IEEE Int. Conf. on Robotics and Automation*, Barcelona, 2005, pp. 4600-4605.
[13] V. Duindam, R. Alterovitz, S. Sastry, and K. Goldberg, "Screw-based motion planning for bevel-tip flexible needles in 3D environments with obstacles," in *2008 IEEE Int. Conf. on Robotics and Automation*, pp. 2483-2488.
[14] J. J. Xu, V. Duindam, R. Alterovitz, and K. Goldberg, "Motion planning for steerable needles in 3D environments with obstacles using rapidly-exploring random trees and backchaining," in *4th IEEE Conf. on Automation Science and Engineering*, 2008, pp. 41-46.
[15] L. A. Lyons, R. J. Webster, and R. Alterovitz, "Motion planning for active cannulas," in *2009 IEEE/RSJ Int. Conf. on Intelligent Robots and Systems*, pp. 801–806.
[16] J. Xiao and R. Vatcha, "Real-time adaptive motion planning for a continuum manipulator," in *2010 IEEE/RSJ Int. Conf. on Intelligent Robots and Systems*, pp. 5919–5926.
[17] G. Ch. Niu, Z. Ch. Zheng, Q. J. Gao, W. J. Wang, and L. Wang, "A novel design of aircraft fuel tank inspection robot," *TELKOMNIKA* , vol. 11, no. 7, pp. 3684-3692, July 2013.
[18] W. Rudin, *Principles of Mathematical Analysis*, 3rd ed., USA: McGraw-Hill, Inc, 1976, pp. 83-97.

**Qingji Gao** received the B.S. degree in computer and application from Wuhan College of Hydraulic and Electrical Engineering, Wuhan, China, in1988, and the M.S. degree in control theory and control engineering from Northeast China Institute of Electric Power Engineering, Jilin, in 1993, and the Ph.D. degree in computer technology and application from the Harbin Institute of Technology, Harbin, in 2006.

From 2003, he has been the director of the Robotics Institute in Civil Aviation University of China, at Tianjin, China. He is a Professor of aviation automation engineering and his research fields include robot vision, situational awareness, intelligent robotics and control systems.

**Zunchao Zheng** received the B.S. degree in information and computing science from Dalian Jiaotong University at Dalian in 2007. Since then, he has been a graduate student for M.S. degree in the Robotics Institute, Civil Aviation University of China, at Tianjin, China.

**Guochen Niu** received the B.S. degree in automation from Northeast Dianli University, Jilin, in 2002 and the M.S. degree in control theory and control engineering from Northeast Dianli University, in 2005. Since 2010, he has been studying for Ph.D. degree in the Robotics Institute, Beihang University, at Beijing, China.

In 2005, he joined the Robotics Institute, Civil Aviation University of China, as a lecturer of automation. His main research interests are mechatronics servo control and learning control.